Journal of Inflammation Research

Dovepress
Taylor & Francis Group

Open Access Full Text Article

ORIGINAL RESEARCH

Ethyl Acetate Extract of *Elsholtzia bodinieri* Vaniot Attenuates Oxidative Stress in ALI Mice

Haiaolong Yin[1,*], Jianhua Hu[2,*], Yaxian Li[1], Yi Feng[1], Zhiwei Li[1], Rongyan Sun[1], Lei Tian[1], Ye Li[3]

[1]Faculty of Food Science and Engineering, Kunming University of Science and Technology, Kunming, 650500, People's Republic of China; [2]Department of Orthopedic Surgery, the First People's Hospital of Yunnan Province, the Affiliated Hospital of Kunming University of Science and Technology, Kunming, 650500, People's Republic of China; [3]School of Medicine, Kunming University of Science and Technology, Kunming, 650500, People's Republic of China

*These authors contributed equally to this work

Correspondence: Lei Tian, Faculty of Food Science and Engineering, Kunming University of Science and Technology, Kunming, 650500, People's Republic of China, Email leotian@kust.edu.cn; Ye Li, School of Medicine, Kunming University of Science and Technology, Kunming, 650500, People's Republic of China, Email liye918@gmail.com

Purpose: Acute lung injury (ALI) is a serious clinical respiratory disease, but there are few effective drugs for ALI. As a natural product, *Elsholtzia bodinieri Vaniot* is used as a drink and medicine in ethnic minority areas of Southwest China. In previous studies, we found that *E. bodinieri* Vaniot methanol extract (EBE) was effective against ALI. This study was carried to investigate the role and mechanisms of EBE ethyl acetate extract (EBEE) against oxidative stress in ALI.

Methods: By multiple bioinformatics analysis, AGER and ITGB2 were found to be the potential target genes of EBEE against oxidative stress in ALI. Different doses of EBEE were feed into ALI mice in vivo (600 mg/kg bw, 200 mg/kg bw) and .RAW 264.7 cells (100 μg/mL, 25 μg/mL) in vitro to evaluate the protection function. Western Blot, immunofluorescence and biochemical factor detection were used to measure the levels of oxidative stress associated factors, and gut microbiota analysis examined the gut microbiota in mice.

Results: EBEE, which contained a total of 1374 components, was identified as the most active against oxidative stress. The EBEE treatment most significantly downregulated the ROS, MDA and pathological damages. AGER and ITGB2 were picked up as target genes of EBEE against ALI by bioinformatics. In vitro and in vivo, AGER, NOX4, and P-GSK3β expression levels were significantly decreased, and ITGB2, P-AKT, NRF2 and HO-1 were significantly up-regulated throughout EBEE treatment. By consuming EBEE, *Chthoniobacteraceae* significantly increased, while the pernicious bacteria *Staphylococcaceae* significantly reduced in ALI mouse.

Conclusion: EBEE treatment significantly ameliorated the pathological damage and oxidative stress by regulating AGER, ITGB2 and related pathways in vitro and in vivo. Furthermore, EBEE treatment improved the composition of the gut microbiota in ALI mice. These data suggested that EBEE could be used as a potential functional food for prevention and treatment of ALI.

Keywords: *Elsholtzia bodinieri* Vaniot, ethyl acetate extract, acute lung injury, oxidative stress, AGER, ITGB2

Introduction

E. bodinieri Vaniot is a perennial herb of the Labiatae family, widespread in Yunnan and Guizhou at altitudes of 1200–1300 metres and has many common names such as "Dongzisu" and "Toothbrush Grass" in Yunnan, China.[1] *E. bodinieri* Vaniot has a wide range of uses, not only as a medicine to take but also as a drink in ethnic minority areas. It can be used as a traditional Chinese medicine to treat hepatitis, cough, pharyngitis, headache and fever.[2] Yang et al found that several triterpenoid saponins isolated from the n-BuOH extract of the aerial part of *E. bodinieri* Vaniot showed anti-influenza activity.[3] In previous research, our team extracted and identified nine major compounds from *E. bodinieri* Vaniot (EBE), including 6 flavonoids and 3 phenols. We then investigated the effect of EBE in ameliorating acute lung injury in vivo and in vitro and found that EBE treatment inhibited pyroptosis, attenuated inflammation, alleviated oxidative stress and induced macrophage polarization towards the M2 phenotype.[1,4] However, further research is needed to determine which components of *E. bodinieri* Vaniot fraction play a role and what mechanisms are involved in alleviating oxidative stress in ALI.

Received: 24 February 2025
Accepted: 31 May 2025
Published: 6 June 2025

ALI, a disease characterised by inflammation and oxidative damage,[5] is manifested by immune cell infiltration in the lungs, acute hypoxic respiratory failure, and hypoxemia without left atrial hypertension.[6,7] ALI can be caused by a variety of factors, such as induction by lipopolysaccharide (LPS),[8,9] methicillin-resistant *Staphylococcus aureus*,[10] and some diseases can cause the subsequent development of ALI, such as COVID-19,[11] sepsis,[12] influenza A,[13] haemorrhagic shock[14] and so on. ALI complications can also occur after video-assisted thoracoscopic surgery.[15] In addition, cigarette smoke can also cause ALI.[16] However, the clinical treatment of ALI is limited,[17] so it can be extremely harmful, it has the characteristics of high morbidity and high mortality,[18] and the state of lung disease affects the function of megakaryocytes and platelets in the body.[19] ALI treatment methods can be divided into two main categories, mechanical ventilation and drug therapy, and the drug commonly used in clinical practice is dexamethasone, but a major drawback of these drugs is that they are associated with harmful side effects such as osteoporosis and gastric ulcers.[20] Given the severity of the damage it causes, there is a need to develop a natural plant product that can alleviate ALI. From our previous studies, we have found that *E. bodinieri* Vaniot could alleviate ALI,[1,4] however it is not yet known whether each fraction of the EBE has the effect of inhibiting ALI and which fraction has a major antioxidant stress effect in the treatment of ALI. Oxidative stress, usually caused by excessive reactive oxygen species (ROS), can occur in some situations such as ageing, infection and systemic disease.[21–23]

In this study, we found that EBEE (one of the EBE fractions) had a greater antioxidant capacity than other fractions, EBEE treatment significantly ameliorated the pathological damage and oxidative stress in the lung tissue of ALI mice, and AGER and ITGB2 were screened as possible pharmacological targets of EBEE against oxidative stress in ALI based on several bioinformatics databases, EBEE treatment attenuated oxidative stress by regulating AGER, ITGB2 and related pathways were verified in vitro and in vivo, EBEE treatment improved the composition of the gut microbiota in ALI mice.

Materials and Methods

Extraction and Identification of E. bodinieri Vaniot Fractions

Previously, *E. bodinieri* Vaniot was collected from Wenshan, Yunnan Province, China, and was identified by Professor Cao, voucher specimen deposited at the Faculty of Food Science and Engineering, KUST.[4] The collection and extraction of EBE were described in detail in our previous study,[4] in brief, the powdered *E. bodinieri* Vaniot was degreased with petroleum ether and extracted three times with an aqueous solution of 80% methanol by means of ultrasonic extraction, each time for 30 minutes (material/solution ratio 1:10). It was centrifuged at 1500g for 10 minutes to obtain the supernatant, which was then evaporated and lyophilised under vacuum to obtain EBE. EBE was dissolved in distilled water at a solid-liquid ratio of 1:10[24] and extracted sequentially with ethyl acetate, butanol, and dichloromethane using a liquid-liquid partition method (v/v; 1:1), with each solvent being extracted three times. After evaporation and lyophilization, EBEE, EBE dichloromethane extract (EBED), EBE butanol extract (EBEB) and residual EBE aqueous extract (EBEW) were obtained. EBE and these fractions were identified using a widely targeted components analysis approach.

Evaluation of Antioxidant Activity

EBEW, EBEE, EBED, and EBEB were dissolved in the DMEM/high glucose (8123269, Gibco, Carlsbad, CA, USA). RAW 264.7 (TIB-71, ATCC, Rockefeller, MA, USA), mouse mononuclear macrophage leukemia cells, were seeded in 96-well plates and divided into Control, DMSO, LPS, EBEE, EBEB, EBED and EBEW groups. After 24 hours of culture, 1μg/mL LPS (L8880, Solarbio, Beijing, China) was added to Model, EBEE, EBEW, EBEB and EBED groups, respectively, and the ROS level of each group was detected 24 hours later using the ROS kit (S0033S, Beyotime, Shanghai, China).

ALI Mice Model

Male C57BL/6J mice (7 weeks old, SPF, Beijing, China) were randomly divided into six groups: Control, DMSO, LPS, EBEE(600), EBEE(200) and DXM groups (six mice in each group). Dimethyl sulfoxide solution (DMSO) was used to accelerate the dissolution of EBEE and this group was established to ensure the uniformity of the experiment. After placing all animals in a constant environment (24°C, moderate humidity, 12 h dark/light cycle) for one week, the Control group received distilled water, the DMSO group received the same amount of DMSO, the EBEE(600) and EBEE(200) groups received 600 mg/kg (body weight) and 200 mg/kg (body weight) EBEE, respectively, and the DXM group

received 10 mg/kg (body weight) dexamethasone (DXM) (D8040, Solarbio, Beijing, China). After the experiment lasted for one week,[25] the Model, EBEE(600), EBEE(200) and DXM groups were injected with LPS (L8880, Solarbio, Beijing, China) at a concentration of 1μg/g (body weight) by nasal drip perfusion and then induced acute lung injury for 24 hours.[26] All mice were fasted for 12 hours, and the blood of mice was collected by ethylenediaminetetraacetic acid venous blood collection using the eyeball extraction method. They were then centrifuged at 3000 rpm for 10 minutes at 4°C, and the plasma was collected and stored. All experimental and animal care protocols were approved by the Kunming University of Science and Technology Animal Ethical Committee (PZWH(Dian) K2022-0006) and the European Community guidelines (EEC Directive of 1986; 86/609/EEC).

Histological Analysis

Mouse lung tissue was embedded in cold 4% paraformaldehyde (BL539A, Biosharp, China) for 2 days and then immersed in a gradient of ethanol to facilitate dehydration. Paraffin-embedded tissue block 4 μm section. Sections were first deparaffinised in xylene and repeated for 20 minutes each time. After rehydration in reduced concentration ethanol solution for 5 min, they were rinsed in water for 5 min. Dye used in the hematoxylin and eosin (H&E) staining techniques. An optical microscope (Olympus, Japan) was used to observe the pathological changes in the lung tissue sections. The edema score of lung tissue was based on the previous literature report.[27]

Exploration and Identification of Key Genes

The target genes of EBEE compounds were predicted from the Swiss Target Prediction database (http://www.swisstargetprediction.ch/).[28] The genes related to ALI were retrieved from DisGeNET (https://www.disgenet.org/).[29] Differentially expressed genes (DEGs) of GSE17355 were analyzed using R. The overlap of EBEE target genes, ALI and DEGs was performed using Venn diagram with the R package. Gene Ontology (GO) and Kyoto Encyclopedia of Genes and Genomes (KEGG) analysis of the overlapping gene were performed using R. The STRING database was used for protein-protein interaction (PPI) analysis of overlapping genes.

Cell Experiments

RAW 264.7 is a leukemic monocyte/macrophage cell line of mouse. Previous studies showed that RAW 264.7 was stimulated with LPS to establish steadily inflammatory model.[1] RAW 264.7 cells were cultured in DMEM/high glucose (8123269, Gibco, Carlsbad, CA, USA), supplemented with 10% fetal bovine serum (04–001-1A, Biological Industries, Kibbutz Beit-Haemek, Israel) and 1% penicillin-streptomycin solution (03–031-1B, Biological Industries, Kibbutz Beit-Haemek, Israel) at 37 °C in 5% CO_2 humidified atmosphere and cells were passaged on time. The cell viability experiment was performed using the Cell Counting Kit-8 (CCK-8) assay (CK04, DOJINDO, Kumamoto, Japan). RAW 264.7 cells were seeded at a density of 4×10^5 cells/well in 6-well plates and were also divided into six groups: Control, DMSO, LPS, EBEE(100), EBEE(25) and DXM groups. The Control group was not treated and the DMSO group was treated with the same amount of DMSO required to dissolve EBEE. The EBEE(100) and EBEE(25) groups were supplemented with 100 μg/mL and 25 μg/mL EBEE in DMEM, respectively, and the DXM group was supplemented with 10μM dexamethasone (D8040, Solarbio, Beijing, China) in DMEM. After 24 hours of incubation, 1μg/mL LPS was added to the LPS, EBEE(100), EBEE(25) and DXM groups. Both LPS and DXM need to be dissolved before use. After a further 24 hours, samples were collected for each group.

Cytokines Detection

The levels of ROS (S0033S, Beyotime, Shanghai, China), Malonaldehyde (MDA) (S0131S, Beyotime, Shanghai, China), Superoxide dismutase (SOD) (A001-3, Nanjingjiancheng, Nanjing, China) and Glutathione (GSH) (A006-2-1, Nanjingjiancheng, Nanjing, China) were determined according to the instructions of the kits. In mouse experiments, plasma ROS levels were measured using the Mouse ROS ELISA Kit (ml009876-1, MLBIO, Shanghai, China). Data were read on a microplate reader (Biotek, Santa Clara, CA, USA) and analyzed using GraphPad Prism 9.0.2.161 software.

Western Blotting

RIPA lysis buffer (R0010, Solarbio, Beijing, China) was used to lyse cells and tissues during sample extraction, 160μL of RIPA containing 1% PMSF was added to each 20mg mice lung tissue, and for cells, 200ul of RIPA containing 1% PMSF was added to each well of the 6-well plate. The BCA protein quantification kit ((P0010, Beyotime, Shanghai, China) was used to detect the protein concentration in the lysis buffer. An equivalent amount of protein was separated by SDS-PAGE (7.5% or 10%) and then transferred to a PVDF membrane (IPVH00010, Millipore, Saint Louis, MO, USA). The primary antibodies used were: AGER (1:5000, 16,346-1-AP, Proteintech, Wuhan, China), NADPH Oxidase 4 (NOX4) (1:2500, 14,347-1-AP, Proteintech, Wuhan, China), Heme Oxygenase 1 (HO-1) (1:2000, 66,743-1-lg, Proteintech, Wuhan, China), Nuclear Factor-like 2 (NRF2) (1:2000, 80,593-1-RR, Proteintech, Wuhan, China), Phosphorylated glycogen synthase kinase 3 beta (P-GSK3β) (1:1000, 14,850-1-AP, Proteintech, Wuhan, China), Glycogen Synthase Kinase 3 beta (GSK3B) (1:5000, 22,104-1-AP, Proteintech, Wuhan, China), Phosphorylated Protein kinase B (P-AKT) (1:10,000, 80,455-1-RR, Proteintech, Wuhan, China), Protein kinase B (AKT) (1:5000, 10,176-2-AP, Proteintech, Wuhan, China), ITGB2 (1:1000, 10,554-1-AP, Proteintech, Wuhan, China), GAPDH (1:10000, HRP-60004, Proteintech, Wuhan, China). And anti-mouse lgG (1:5000, SA00001-1, Proteintech, Wuhan, China) and anti-rabbit lgG (1:10000, SA00001-2, Proteintech, Wuhan, China) were the secondary antibodies. ECL chemiluminescent substrate Reagent Kit (PK10003, Proteintech, Wuhan, China) was used to visualize the bands.

Immunofluorescent Staining

Optimal cutting temperature (O.C.T) compound (SAKURA Tissue-Tek, Japan) was used to embed mouse lung tissue and frozen at −80 °C, followed by rapid sectioning at 15 μm using a freezing microtome (CM 1950, Leica, Germany). These sections were then fixed in 4% paraformaldehyde for 30 minutes and washed three times in phosphate buffer saline (PBS), incubated with 3% H_2O_2 for 10 minutes, rinsed three times with PBS for 5 minutes each, and blocked with 10% goat serum overnight at 4°C. Sections were incubated with NRF2 antibody for 1 hour at 37°C and washed three times with PBS for 5 minutes each. The sections were then incubated for 45 minutes at 37°C with Multi-rAb CoraLite® Plus 488 goat antirabbit recombinant secondary antibody (H+L) (1:200, RGAR002, Proteintech, Wuhan, China). Finally, the sections were washed three times with PBS for 10 minutes each and coverslipped with Fluoroshield containing DAPI (D1306, Invitrogen, USA). A confocal microscope (Leica Microsystems, Germany) was used to observe the section. Images were taken from at least 3 random fields of view in each section and the data were analysed using Image-Pro Plus 6.0.

Gut Microbiota Analysis

Fecal samples were collected and analyzed using 16S rRNA sequencing method. Bacterial DNA was extracted, cloned, and sequenced by Novogene Bioinformatics Technology Co. Ltd. (Tianjin, China). Barcoded primers were used along with genomic DNA to clone the 16S rDNA V3-V4 region. The gene library was constructed and sequenced according to the instructions of Novogene Co, Ltd.

Statistical Analysis

Differences between groups were analyzed using one-way ANOVA followed by Tukey's post hoc test for multiple comparisons (GraphPad Software, San Diego, CA, USA). $P < 0.05$ was considered statistically significant, and the data were presented as the mean ± SEM.

Results

Antioxidant Activity and Compositional Analysis of EBEE

To determine the antioxidant activity of EBE fractions in the LPS-induced inflammation model, ROS levels were measured in each group. ROS levels were upregulated in the LPS group, while EBEE treatment most significantly downregulated ROS (Figure 1A). Therefore, EBEE was selected for further study, and a comparison was made between the components of EBE vs EBEE. The results showed that EBE and EBEE were significantly different in flavonoids, phenolic acids, amino acids and derivatives, lipids, etc. (Figure 1B). A total of 1374 components of

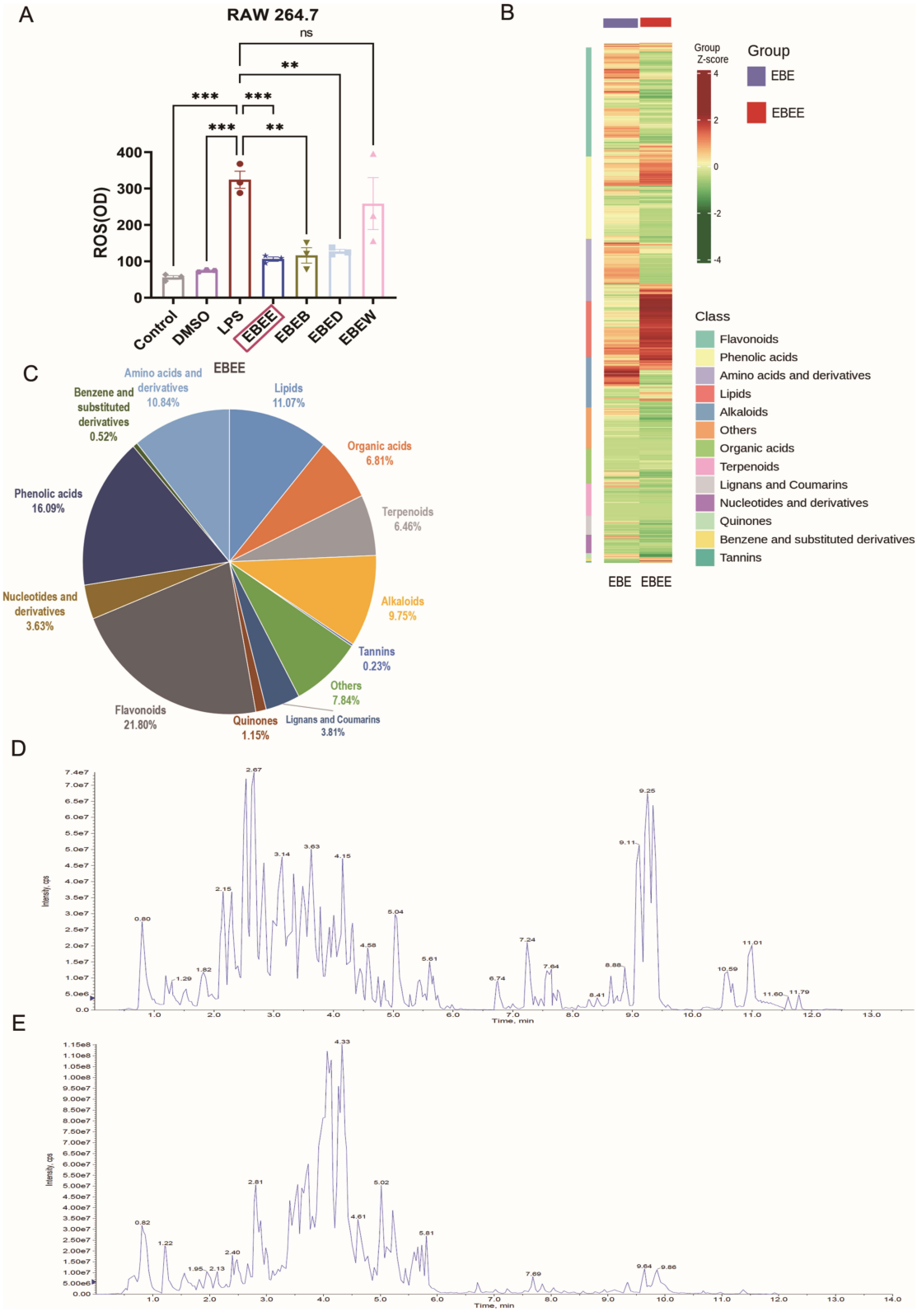

Figure 1 Antioxidant activity and compositional analysis of EBEE. (**A**) The levels of ROS in cell model. (**B**) Cluster heatmap analysis on components of EBE vs EBEE (**C**) The content of EBEE compounds. (**D** and **E**) The positive and negative total ion chromatograms of the components of EBEE. Data are presented as mean ± SEM, n = 3. ns. P > 0.05, ** P < 0.01, *** P < 0.001.

https://doi.org/10.2147/JIR.S522638

EBEE were identified using the Metware database, including 21.8% flavonoids, 16.09% phenolic acids, 10.84% amino acids and their derivatives, 11.07% lipids, 9.75% alkaloids, 6.81% organic acids, 6.46% terpenoids, 3.63% nucleotides and their derivatives, 3.81% lignans and coumarins, 1.15% quinones, 0.52% benzene and its derivatives, 0.23% tannins, and 7.84% others (Figure 1C). The positive and negative total ion chromatograms of the components of EBEE were shown in Figure 1D and E.

EBEE Attenuated the Oxidative Stress of ALI in Mice

EBEE treatment significantly ameliorated the pathological lung tissue damage in the mouse model, similar to the DXM group (Figure 2A). The pulmonary edema score was significantly increased in the LPS group, while EBEE and DXM treatment decreased it (Figure 2B). ROS and MDA, indicators of oxidative stress, were remarkably increased in the LPS group, while administration of EBEE and DXM reduced them (Figure 2C and D).

Exploration and Identification of Target Genes Regulated by EBEE in ALI Mice

Forty-nine overlapping genes were screened from ALI-related genes, potential EBEE target genes and DEGs of GSE17355 (Figure 3A). The most enriched GO terms of overlapping genes were shown in Figure 3B, and the top 20 KEGG pathways of overlapping genes were shown in Figure 3C, which included calcium signaling pathway, age-rage signaling pathway and so on. Partially overlapping genes were marked in the Calcium signaling pathway (Figure 3D) and the Age-rage signaling pathway (Figure 3E) by R. The PPI network of overlapping genes was visualized using Cytoscape software (Figure 3F). Based on these analyses, AGER and ITGB2 could be the potential target genes of EBEE protect against ALI.

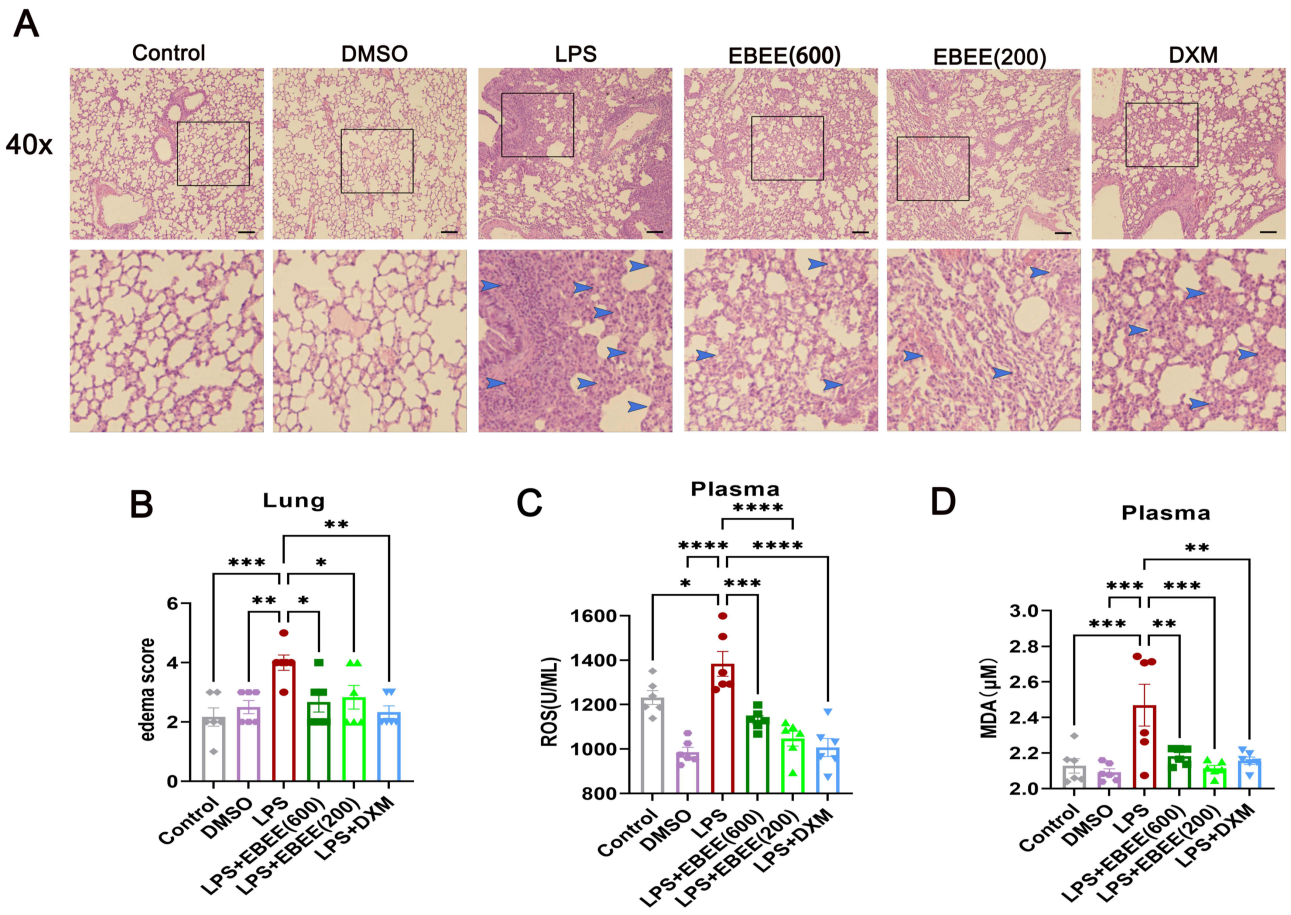

Figure 2 EBEE attenuated the oxidative stress of ALI in Mice. (**A**) Representative H&E staining of mouse lung tissue, blue arrows indicate pathological lesions. Scale bars were 100μm. (**B**) The effects of EBEE on the edema score of mouse lung tissue. (**C** and **D**) The effects of EBEE on the ROS and MDA levels of mouse plasma. Data are presented as mean ± SEM, n = 6. *P < 0.05, **P < 0.01, ***P < 0.001, ****P < 0.0001.

 https://doi.org/10.2147/JIR.S522638

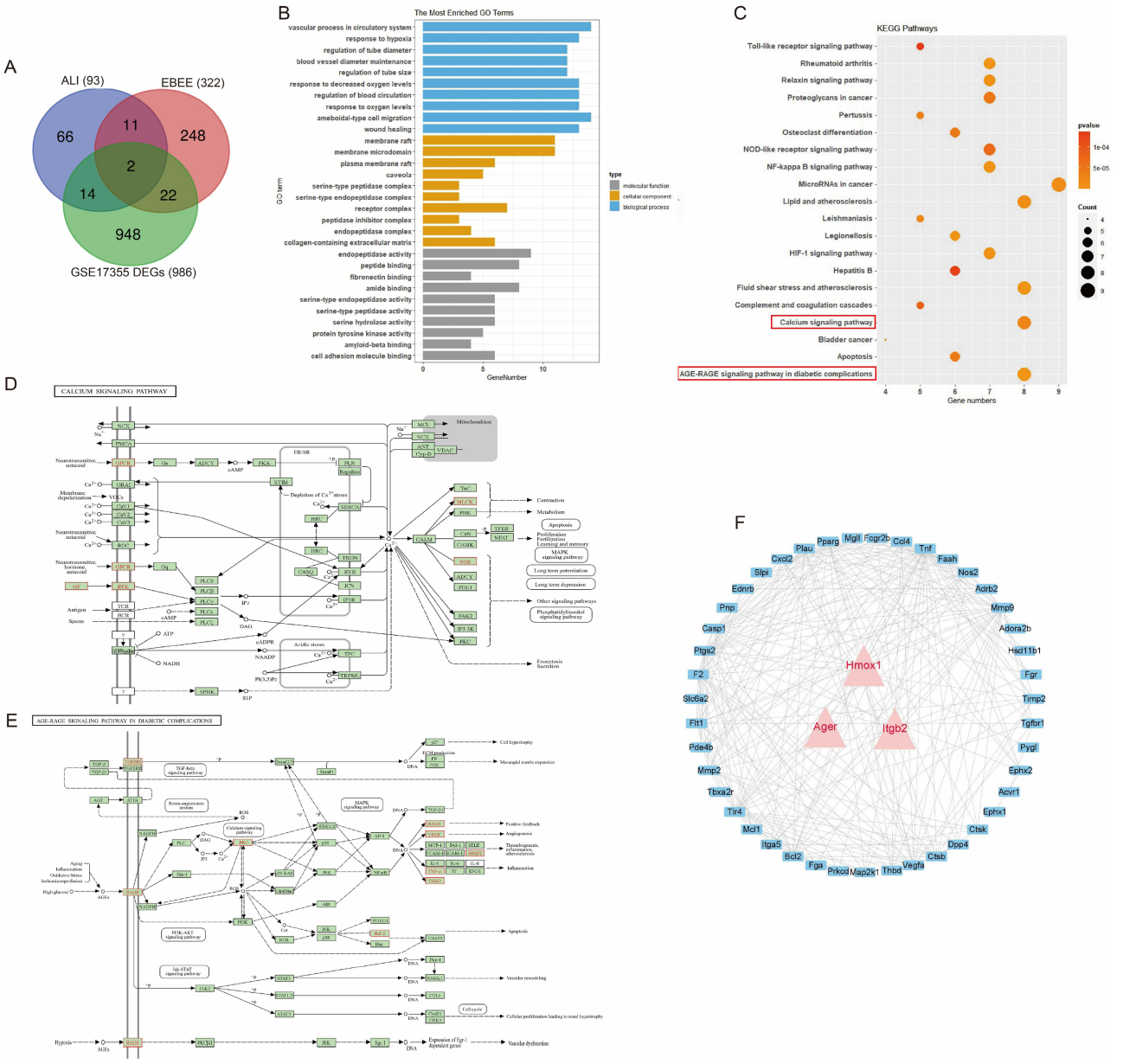

Figure 3 Exploration and identification of target genes regulated by EBEE in ALI mice. (**A**) Venn diagram of overlapping genes. (**B**) The top 30 enriched terms of overlapping genes were identified by GO analysis. (**C**) The top 20 KEGG pathways of overlapping genes. (**D**) Partially overlapping genes were marked in the Calcium signaling pathway. (**E**) Partially overlapping genes were marked in the Age-rage signaling pathway. (**F**) PPI network of overlapping genes. The blue and pink nodes represent overlapping genes, the edges represent the interactions between them.

Validation of Target Genes, Associated Pathways and Antioxidant Activity in the Cell Model

Gradient concentrations of EBEE were measured using CCK-8 at different times to examine the effect on cells. Subsequently, 100 μg/mL and 25 μg/mL EBEE were used to investigate the effects on the cell model (Figure 4B). To verify the target genes and pathways of EBEE against ALI, the levels of related factors were determined in the cell model. AGER and NOX4 levels were significantly increased in the LPS group, while EBEE treatment sharply decreased them (Figure 4D and E). It has been reported that NOX4, as a member of the NADPH oxidase family of enzymes, can produce ROS that can cause oxidative stress,[30,31] and excessive ROS would produce MDA.[32,33] In the LPS group, the levels of ITGB2, P-AKT, NRF2 and HO-1 were significantly down-regulated, whereas

https://doi.org/10.2147/JIR.S522638

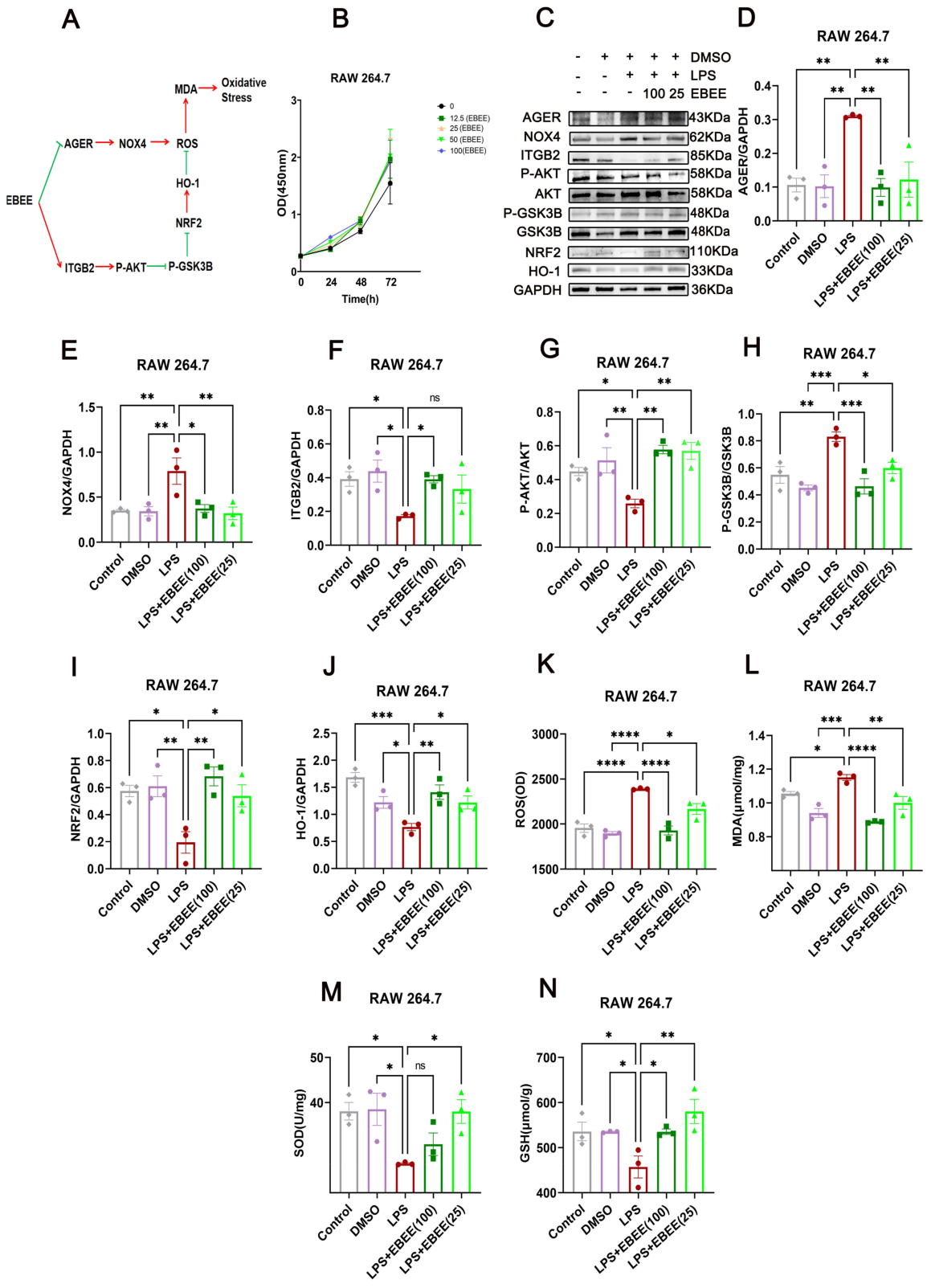

Figure 4 Validation of target genes, associated pathways and antioxidant activity in the cell model. (**A**) Illustration of the mechanism of action of the EBEE. (**B**) The effect of several concentrations of EBEE on RAW 264.7 viability at different times. (**C–J**) Western blot analyses of AGER, NOX4, ITGB2, P-AKT, P-GSK3β, NRF2, HO-1 expression in the cell model. (**K-N**) The effects of EBEE on ROS, MDA, SOD, and GSH levels in the cell model. Data are presented as mean ± SEM, n = 3. ns P > 0.05, *P < 0.05, **P < 0.01, ***P < 0.001, ****P < 0.0001.

administration of EBEE up-regulated them all (Figure 4F, G, I and J). HO-1 has been reported to be an antioxidant enzyme that resists oxidative stress,[34,35] and its upregulation may lead to the disruption of ROS, including lipROS, cytoROS, and mtROS homeostasis.[36] P-GSK3β, ROS and MDA levels were obviously increased in the LPS group, but EBEE treatment decreased them all (Figure 4H, K and L). In addition, the contents of SOD and MDA were significantly reduced in the LPS group, administration of EBEE restored them (Figure 4M and N). SOD has been reported to be one of the antioxidant enzyme systems,[37] and GSH has been reported to be one of the antioxidants that protect the mitochondrial system from oxidative damage.[38] Taken together, EBEE restrained oxidative stress by regulating AGER, ITGB2 and related pathways in the cell model.

EBEE Attenuated Oxidative Stress by Regulating AGER, ITGB2 and Related Pathways in ALI Mice

To explore the mechanism of EBEE antioxidation in ALI mice, the target genes and pathway proteins were detected in lung tissue. In the LPS group, the expression of AGER, NOX4 and P-GSK3β were significantly up-regulated, whereas EBEE administration significantly down-regulated them (Figure 5C, D and H). On the contrary, ITGB2, P-AKT, NRF2 and HO-1 levels were significantly down-regulated in the LPS group and up-regulated by EBEE treatment (Figure 5E, F, I and J). Representative immunofluorescence staining and data of NRF2 in lung tissue as shown in Figure 5G and I. These data indicated that EBEE treatment attenuated oxidative stress by regulating AGER, ITGB2 and related pathways in ALI mice.

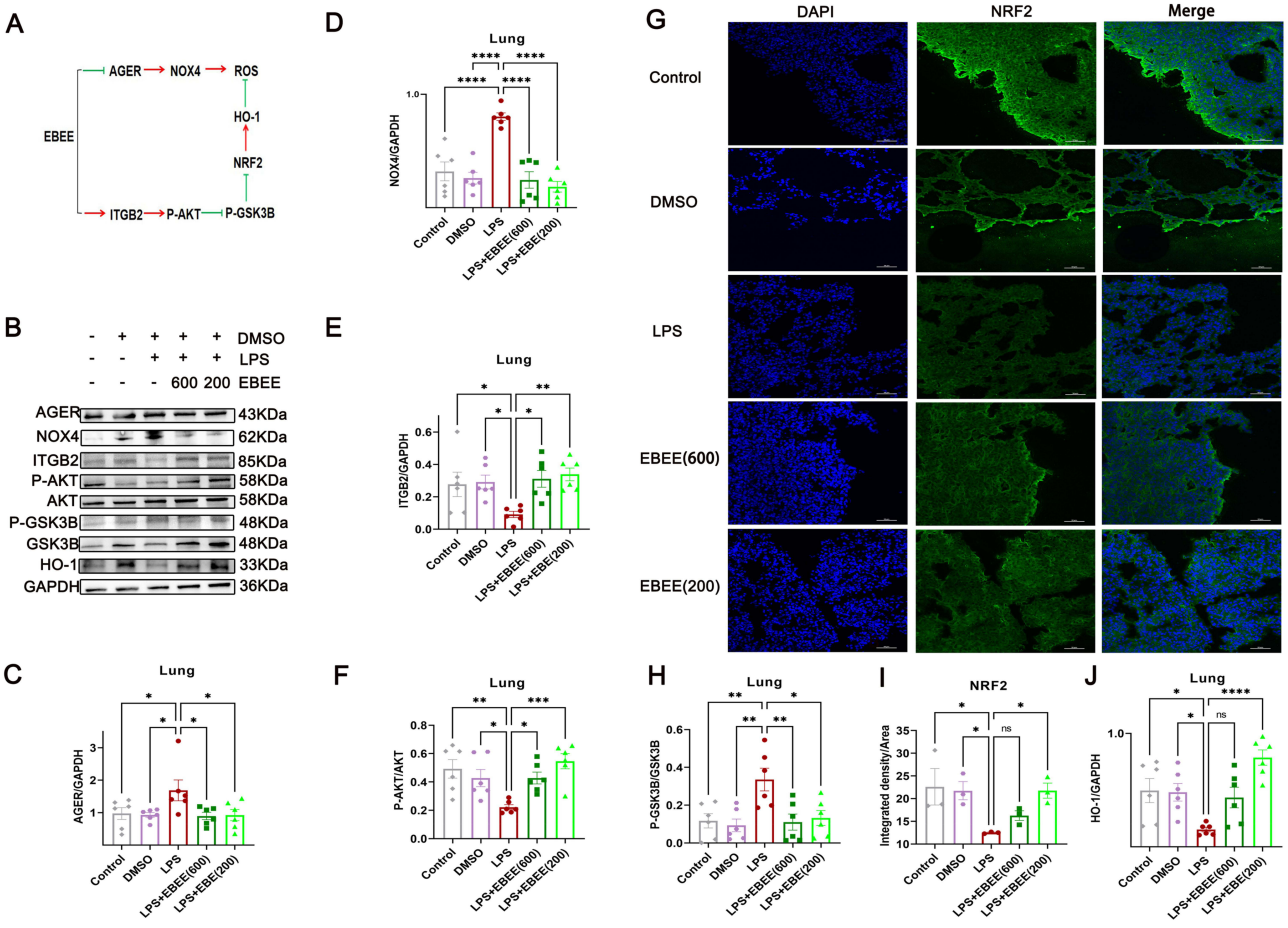

Figure 5 EBEE attenuated oxidative stress by regulating AGER, ITGB2 and related pathways in ALI mice. (**A**) The pathways of EBEE regulating oxidative stress in the ALI mouse model. (**B-F, H, J**) Western blot analyses of AGER, NOX4, ITGB2, P-AKT, P-GSK3B, HO-1 expression in the ALI mouse model. (**G** and **I**) Representative immunofluorescence staining of NRF2 in lung tissues. Scale bars, 10 μm. Data are presented as mean ± SEM, n = 6 (immunofluorescence staining n=3). ns P > 0.05, *P < 0.05, **P < 0.01, ***P < 0.001, ****P < 0.0001.

https://doi.org/10.2147/JIR.S522638

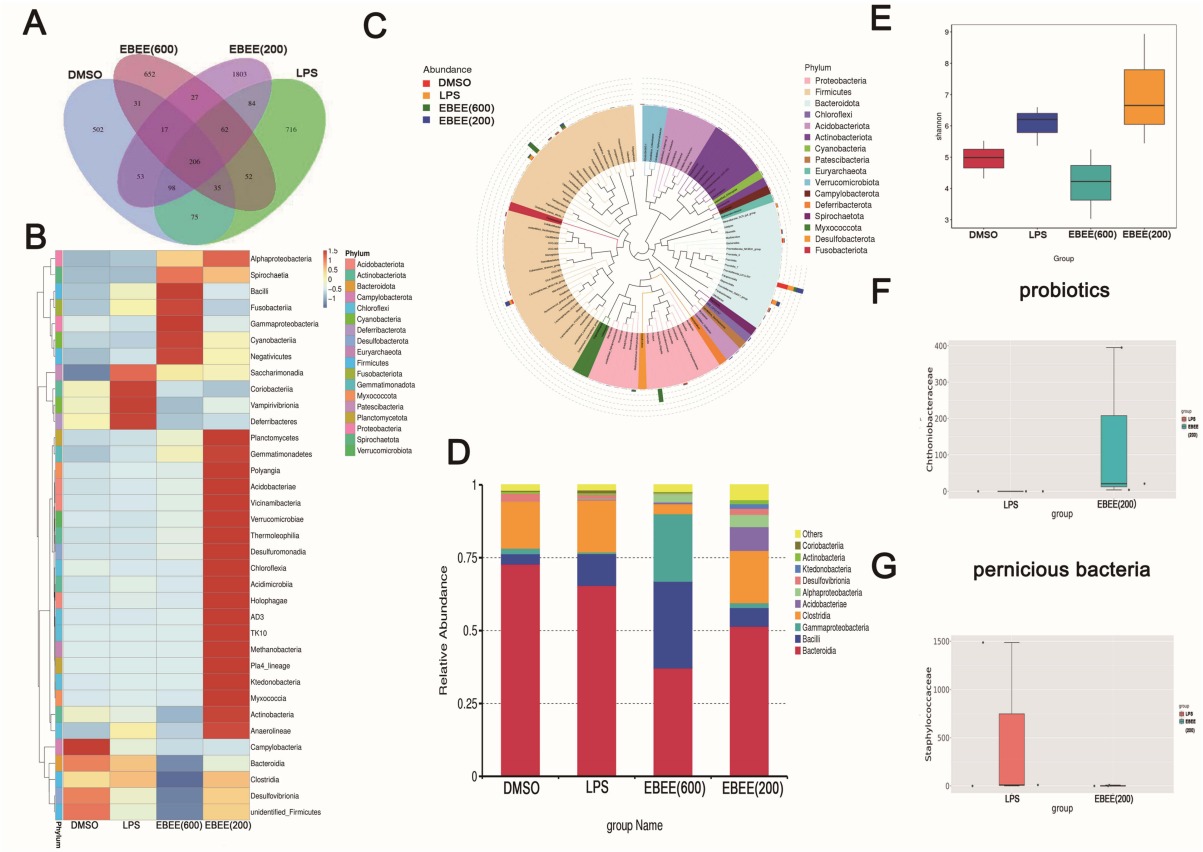

Figure 6 EBEE improved gut microbiota composition in ALI mice. (**A**) Venn diagram of OTUs in each group. (**B**) The heat map of the gut microbiota at the class level. (**C**) Relative abundance of gut microbiota at the genus level. (**D**) Relative abundance of gut microbiota the at the class level. (**E**) Differential analysis of Shannon indices. (**F**) *Chthoniobacteraceae* relative abundance. (**G**) *Staphylococcaceae* relative abundance, n = 3.

EBEE Improved Gut Microbiota Composition in ALI Mice

To further investigate the effect of EBEE on the gut microbiota in the ALI mouse model, 16S rDNA from mouse faeces was analyzed. The Venn diagram was shown in Figure 6A, which exhibited that there were 206 operational taxonomic units (OTUs) for all samples, and the DMSO, LPS, EBEE(600), and EBEE(200) groups had 502, 716, 652, and 1803 unique OTUs, respectively. The heat map of the gut flora at the class level was shown in Figure 6B. The top 100 species of gut bacteria at the genus level were shown in Figure 6C, and the relative abundance of the top 10 microbial flora at the class level was shown in Figure 6D. The Shannon index showed that the value of the LPS group increased, while the administration of EBEE (600) decreased it (Figure 6E). By consuming EBEE (200), probiotics in the intestine of mice, such as *Chthoniobacteraceae*, were significantly higher than those in the Model group, while pernicious bacteria, such as *Staphylococcaceae*, were significantly lower than those in the Model group (Figure 6F and G). In conclusion, EBEE treatment ameliorated the intestinal microbiota composition in ALI mice.

Discussion

Natural compounds and the whole method of Traditional Chinese Medicine, rooted in 3500 years of history, complement each other.[39] Natural products are characterized by diversity, structural complexity and historical therapeutic significance, with considerable biological activity and functional properties.[40] Therefore, reports of various natural product properties such as antioxidant,[41,42] anti-inflammatory,[43–45] anti-fatigue[46] and anti-tumor[47] have become more frequent in recent years. It has become a trend to find pharmaceuticals from natural products that can resist some certain diseases. Due to the severity of the damage caused by ALI and the fact that ALI treatment is not very effective, it remains difficult to find an effective pharmacological treatment that significantly reduces mortality from ALI.[48] In particular, dexamethasone,

a commonly used clinical drug for ALI, may have some side effects.[20] Therefore, there is a need for the discovery of a natural product drug that can be effective against ALI.

We had found that EBEE had the best antioxidant activity in the EBE fractions through experiments in vitro. Component analysis showed that the flavonoid content of EBEE was the highest, and according to existing reports, natural flavonoids in vegetables, fruits and herbs have antioxidant and anti-inflammatory properties.[49,50] EBEE contains a large number of flavonoid compounds, providing a good explanation for EBEE's antioxidant activity; however, the specific functional components and mechanisms is needed further research. ROS are thought to induce oxidative stress and have always been an indicator of oxidative stress.[51] In the mouse model, EBEE treatment significantly reduced ROS and MDA levels and ameliorated the pathological lung tissue damage. However, the mechanism of EBEE on antioxidant activity in the ALI mouse model needs to be further investigated.

We then used bioinformatics analysis to explore and identify the target genes and associated pathways, using several databases and software such as Swiss Target Prediction, DisGeNET, GO, KEGG, STRING and Cytoscape. After considering these analyses, we identified AGER and ITGB2 as potential target genes that are regulated by EBEE in the ALI mouse. AGER has been reported to be associated with lung injury and inflammatory diseases,[52] and ITGB2 has also been found as a potential therapeutic target for inflammatory bowel disease.[53] Subsequently, we verified that EBEE treatment restrained oxidative stress by regulating AGER, ITGB2 and related pathways in vitro and in vivo. The roles of AGER in many inflammatory diseases such as diabetes are mainly due to the accumulation of advanced glycosylation end products in pathological states, which results in the continuous overexpression of AGER.[54] AGER can specifically identify and interacts with advanced glycation end products (AGEs), other endogenous ligands and epigenetic mediators.[55] ITGB2 could act as a central hub gene associated inflammation, it is often closely related to the infiltration of various immune cells and high expression of ITGB2 is accompanied by immune activation.[56] As a result of our study, EBEE treatment downregulated the expression of AGER and upregulated the expression of ITGB2. However, the current study had some limitations. The specific effect and mechanism of EBEE affects target genes AGER and ITGB2 have yet to plumb the depths of this issue at this time. More research is necessary to further determine which chemical compounds of EBEE can improve the ALI by regulation of AGER and ITGB2.

Afterwards, we investigated the effect of EBEE on the gut microbiota in the ALI mouse model. EBEE treatment improved gut microbiota composition at the class and genus levels in ALI mice. A probiotic, *Chthoniobacteraceae*, was significantly increased, while the harmful bacteria, *Staphylococcaceae*, was significantly decreased after consumption of EBEE in the ALI mouse model. *Chthoniobacteraceae* has been explained to be related to algae growth.[57] Several species of *Staphylococcaceae* are pathogenic, eg *Staphylococcus aureus* is usually associated with wound and surgical infections, pyoderma and otitis, while *Staphylococcus pseudintermedius* is an opportunistic pathogen.[58] These experiments confirmed that EBEE ameliorated gut microbiota composition in ALI mice. EBEE contained numerous active compounds that attenuated the oxidative stress of ALI by regulating potential targets and related signaling pathways, and it's a deeper discovery based on our previous research. However, further research is needed to fully understand the role of these mechanistic pathways in the treatment of ALI and to identify potential targets to prevent ALI progression.

Conclusions

In conclusion, we found that EBEE had the best antioxidant activity, EBEE attenuated oxidative stress by regulating AGER and ITGB2 pathways, and EBEE improved gut microbiota composition in ALI mice. This study provides a new idea for the treatment of ALI through pharmaceutical and food homology based on natural products.

Abbreviations

ALI, Acute lung injury; EBEE, *Elsholtzia bodinieri Vaniot* ethyl acetate extract; LPS, Lipopolysaccharide; EBE, *Elsholtzia bodinieri Vaniot* methanol extract; ROS, Reactive oxygen species; AGER, Receptor for Advanced Glycation End Products; CD18, Integrin β2; HO-1, Heme oxygenase-1; EBEW, *Elsholtzia bodinieri Vaniot* water extract; EBED, *Elsholtzia bodinieri Vaniot* dichloride extract; EBEB, *Elsholtzia bodinieri Vaniot* butane extract; DMEM, Dulbecco's modified eagle medium; DMSO, Dimethyl sulfoxide; DXM, Dexamethasone; H&E, Hematoxylin and eosin; EDTA, Ethylene diamine tetraacetic acid; MDA, Malonaldehyde; KEGG, Kyoto Encyclopedia of Genes and

Genomes; PPI, Protein-protein interaction; CCK-8, Cell Counting Kit-8; GSH, Glutathione; SOD, Superoxide Dismutase; NO, Nitric oxide; ELISA, Enzyme-linked immunosorbent assay; RIPA, Radio Immunoprecipitation Assay; BCA, Bicinchoninic acid; SDS-PAGE, sodium dodecyl sulfate polyacrylamide gel electrophoresis; PVDF, Polyvinylidene fluoride; NOX4, NADPH Oxidase 4; HO-1, Heme Oxygenase 1; NRF2, Nuclear factor-like 2; GSK3B, Phospho-glycogen synthase kinase 3 beta; P-AKT, Phospho-v-akt murine thymoma viral oncogene homolog 1; GAPDH, Glyceraldehyde-3-phosphate dehydrogenase; ECL, Electrochemiluminescence; OCT, Optimal cutting temperature; PBS, Phosphate Buffered Saline; DAPI, 4′,6-Diamidino-2-Phenylindole; DNA, Deoxyribonucleic acid; PCR, Polymerase chain reaction; GO, Ontology; DEGs, Differentially expressed genes; OTUs, Operational taxonomic units.

Acknowledgments

This research was supported by the National Natural Science Foundation of China (32160106) and Yunnan International Science and Technology Commissioner (202403AK140006).

Disclosure

No potential conflict of interest was reported by the authors.

References

1. Jin S, Xiaoqian J, Yuxu C, et al. Elsholtzia bodinieri Vaniot Ameliorated acute lung injury by NQO1, BCL2 and PTGS2 in silico and in vitro analyses. *Int J Mol Sci*. 2022;23(24):15651. doi:10.3390/ijms232415651
2. Jin-Dong Z, Yue F, Hong-Mei L, Xue-Shan X, Rong-Tao L. A new flavonoid glycoside from Elsholtzia bodinieri. *Nat Prod Res*. 2016;30 (20):2278–2284. doi:10.1080/14786419.2016.1164698
3. Linyao Y, Jiangchao D, Rongtao L, Fei Y, Jindong Z, Bodiniosides S–Y. Seven new Triterpenoid Saponins from Elsholtzia bodinieri and their anti-influenza activities. *Molecules*. 2021;26(21):6535. doi:10.3390/molecules26216535
4. Xiaoqian J, Jin S, Shancheng G, et al. Elsholtzia bodinieri Vaniot ameliorated acute lung injury in mice by regulating pyroptosis, inflammation, oxidative stress and macrophage polarization. *J Ethnopharmacol*. 2023;307:116232. doi:10.1016/j.jep.2023.116232
5. Lei X, Liu X, Yu J, et al. 3-methyladenine ameliorates acute lung injury by inhibiting oxidative damage and apoptosis. *Heliyon*. 2024;10(13): e33996. doi:10.1016/j.heliyon.2024.e33996
6. Rubenfeld GD, Ellen C, Eve P, et al. Incidence and outcomes of acute lung injury. *New Engl J Med*. 2005;353(16):1685–1693. doi:10.1056/NEJMoa050333
7. Nadeem A, Al-Harbi NO, Ahmad SF, et al. Blockade of interleukin-2-inducible T-cell kinase signaling attenuates acute lung injury in mice through adjustment of pulmonary Th17/Treg immune responses and reduction of oxidative stress. *Int Immunopharmacol*. 2020;83:106369. doi:10.1016/j.intimp.2020.106369
8. Yakut S, Gelen V, Kara H, Özkanlar S, Yeşildağ A. Silver Nanoparticles Loaded With Oleuropein Alleviates LPS-Induced Acute Lung Injury by Modulating the TLR4/P2X7 Receptor-Mediated Inflammation and Apoptosis in Rats. *Environ Toxicol*. 2024;39(11):4960–4973. doi:10.1002/tox.24369
9. Han S, Mei S, Lai M, et al. The effect of ethanol extracts of Loulu flower on LPS-induced acute lung injury in mice. *J Ethnopharmacol*. 2024;334:118515. doi:10.1016/j.jep.2024.118515
10. Wu Y, He S, Zhang Y, et al. Sophoricoside ameliorates methicillin-resistant Staphylococcus aureus-induced acute lung injury by inhibiting Bach1/Akt pathway. *Phytomedicine*. 2024;132:155846. doi:10.1016/j.phymed.2024.155846
11. Shin M, Kazuki S, Kohsuke K, et al. Prediction of acute lung injury assessed by chest computed tomography, oxygen saturation/fraction of inspired oxygen ratio, and serum lactate dehydrogenase in patients with COVID-19. *J Infect Chemother*. 2023;30(5):406–416. doi:10.1016/j.jiac.2023.11.013
12. Khalifa MM, Bastawy NA, Rashed LA, Hassan HA, Maksoud OMA, Hassan FE. Berberine protects against sepsis-related acute lung injury in rats via PPAR-γ signaling pathway upregulation and improvement at the cellular level: functional, biochemical, and immunohistochemistry study. *Gen Physiol Biophys*. 2024;43(4):353–366. doi:10.4149/gpb_2024008
13. Wang X, Geng Z, Bao Y, et al. Shufeng Jiedu capsule alleviates influenza A (H1N1) virus induced acute lung injury by regulating the lung inflammatory microenvironment. *Heliyon*. 2024;10(12):e33237. doi:10.1016/j.heliyon.2024.e33237
14. Lian P, Huan Z, Wang Y, Yao H, Han S, Ge X. Protective effect of 8-Gingerol, a potent constituent of ginger, on acute lung injury following hemorrhagic shock in rats. *Exp Anim*. 2024;73(4):446–457. doi:10.1538/expanim.23-0178
15. Zhang Y, Zha T, Song G, et al. Unveiling the protective role of sevoflurane in video-assisted thoracoscopic surgery associated-acute lung injury: inhibition of ferroptosis. *Pulm Pharmacol Ther*. 2024;86:102312. doi:10.1016/j.pupt.2024.102312
16. Joufi FAA, Shaukat S, Hussain L, et al. Lavandula stoechas significantly alleviates cigarette smoke-induced acute lung injury via modulation of oxidative stress and the NF-κB pathway. *Food Biosci*. 2024;59:103834. doi:10.1016/j.fbio.2024.103834
17. Zou Y, Wang X, Chen P, et al. Fragment-based anti-inflammatory agent design and target identification: discovery of AF-45 as an IRAK4 inhibitor to treat ulcerative colitis and acute lung injury. *J Med Chem*. 2024;67(13):10687–10709. doi:10.1021/acs.jmedchem.4c00202
18. Wu W, He Y, Lin D, et al. Dexmedetomidine mitigates lipopolysaccharide-induced acute lung injury by modulating heat shock protein A12B to inhibit the toll-like receptor 4/nuclear factor-kappa B signaling pathway. *Chem Biol Interact*. 2024;398:111112. doi:10.1016/j.cbi.2024.111112
19. Hua T, Zhang G, Yao Y, Jia H, Liu W. Research progress of megakaryocytes and platelets in lung injury. *Annals of Medicine*. 2024;56(1):2362871. doi:10.1080/07853890.2024.2362871

20. Gao B, Qian X, Guo Y, et al. Essential oil from Chimonanthus nitens Oliv. leaves ameliorate inflammation and oxidative stress in LPS-induced ALI through NF-κB and Nrf2 signaling pathways. *J Ethnopharmacol*. 2024;333:118470. doi:10.1016/j.jep.2024.118470
21. Brenner C, Galluzzi L, Kepp O, Kroemer G. Decoding cell death signals in liver inflammation. *J Hepatol*. 2013;59(3):583–594. doi:10.1016/j.jhep.2013.03.033
22. Ansari MY, Ahmad N, Haqqi TM. Oxidative stress and inflammation in osteoarthritis pathogenesis: role of polyphenols. *Biomed Pharmacother*. 2020;129:110452. doi:10.1016/j.biopha.2020.110452
23. Rajizadeh MA, Hosseini MH, Bahrami M, et al. High-intensity intermittent training ameliorates methotrexate-induced acute lung injury. *BMC Pulm Med*. 2024;24(1):45. doi:10.1186/s12890-024-02853-w
24. Guo T, Wei L, Sun J, Hou C-L, Fan L. Antioxidant activities of extract and fractions from tuber indicum cooke & Massee. *Food Chem*. 2011;127(4):1634–1640. doi:10.1016/j.foodchem.2011.02.030
25. Ge R, Su Q, Liang J, Zheng L, Qs L, Tang L. Dulcitol ameliorates LPS-induced acute lung injury (ALI) in mice by inhibiting TLR4/NF-κB activation. *J Funct Foods*. 2025;128:106797. doi:10.1016/j.jff.2025.106797
26. Yuxian G, Yaru L, Shihao Z, et al. Oxidative stress-induced FABP5 S-glutathionylation protects against acute lung injury by suppressing inflammation in macrophages. *Nat Commun*. 2021;12(1):7094. doi:10.1038/s41467-021-27428-9
27. Hrusch CL, Manns ST, Bryazka D, et al. ICOS protects against mortality from acute lung injury through activation of IL-5+ ILC2s. *Mucosal Immunol*. 2018;11(1):61–70. doi:10.1038/mi.2017.42
28. Li WH, Han JR, Ren PP, Xie Y, Jiang DY. Exploration of the mechanism of Zisheng Shenqi decoction against gout arthritis using network pharmacology. *Comput Biol Chem*. 2021;90:107358. doi:10.1016/j.compbiolchem.2020.107358
29. Janet P, Àlex B, Núria Q-R, et al. DisGeNET: a comprehensive platform integrating information on human disease-associated genes and variants. *Nucleic Acids Res*. 2017;45(D1):D833–D839. doi:10.1093/nar/gkw943
30. Dzubanova M, Bond JM, Craige SM, Tencerova M. NOX4-reactive oxygen species axis: critical regulators of bone health and metabolism. *Front Cell Develop Biol*. 2024;12:1432668. doi:10.3389/fcell.2024.1432668
31. Kim JH, Hwang KH, Kim SH, et al. Particulate matter-induced neurotoxicity: unveiling the role of NOX4-mediated ROS production and mitochondrial dysfunction in neuronal apoptosis. *Int J Mol Sci*. 2024;25(11):6116. doi:10.3390/ijms25116116
32. Mamane S, Néziha G-B, Wafa G, et al. Malondialdehyde content and circadian variations in brain, kidney, liver, and plasma of mice. *Chronobiol Int*. 2007;24(4):671–685. doi:10.1080/07420520701535720
33. Francesca G, Valentina F, Salvatore A, et al. Fate of melatonin orally administered in preterm newborns: antioxidant performance and basis for neuroprotection. *J Pineal Res*. 2023;76(1):e12932. doi:10.1111/jpi.12932
34. Mingyi Z, Huiming G, Jimei C, et al. 5-aminolevulinic acid combined with sodium ferrous citrate ameliorates H2O2-induced cardiomyocyte hypertrophy via activation of the MAPK/Nrf2/HO-1 pathway. *Am J Physiol Cell Physiol*. 2015;308(8):C665–C672. doi:10.1152/ajpcell.00369.2014
35. ChienChung Y, LiDer H, ChenYu W, et al. HO-1 upregulation by Kaempferol via ROS-dependent Nrf2-ARE cascade attenuates lipopolysaccharide-mediated intercellular cell adhesion molecule-1 expression in human pulmonary Alveolar Epithelial cells. *Antioxidants*. 2022;11(4):782. doi:10.3390/antiox11040782
36. Hui C, Ping N, Jingling L, et al. Cyclophosphamide induces ovarian granulosa cell ferroptosis via a mechanism associated with HO-1 and ROS-mediated mitochondrial dysfunction. *Jovarian Res*. 2024;17(1):107. doi:10.1186/s13048-024-01434-z
37. Liao MF, Chen CC, Hsu MH. Evaluation of the serum antioxidant status in asthmatic children. *Acta Paediat Taiwan*. 2004;45(4):213–217.
38. Leirós M, Rateb ME, Houssen W, et al. Evaluation of derived compounds from sponges against induced oxidative stress in cortical neurons. *Front Mar Sci*. 2014;12(2):700–718. doi:10.3389/conf.fmars.2014.02.00059
39. Yuhao W, Shenghua C, Jueying C, Shate X, Rongrong S, Xiangfeng S. Targeting ferroptosis regulators in lung cancer: exploring natural products. *Heliyon*. 2024;10(14):e33934. doi:10.1016/j.heliyon.2024.e33934
40. Jiang X, Shon K, Li X, et al. Recent advances in identifying protein targets of bioactive natural products. *Heliyon*. 2024;10(13):e33917. doi:10.1016/j.heliyon.2024.e33917
41. Shenke B, Shuai Z, Shengbao C, Junjie Y, Linyan Z. The profiles of free, esterified and insoluble-bound phenolics in peach juice after high pressure homogenization and evaluation of their antioxidant capacities, cytoprotective effect, and inhibitory effects on α-glucosidase and dipeptidyl peptidase-IV. *Food Chem X*. 2023;21:101092. doi:10.1016/j.fochx.2023.101092
42. Yilin S, Yuanyue Z, Nan M, Shengbao C. Rhus chinensis mill. fruits alleviate liver injury induced by isoniazid and rifampicin through regulating oxidative stress, apoptosis, and bile acid transport. *J Ethnopharmacol*. 2023;310:116387. doi:10.1016/j.jep.2023.116387
43. Yan FS, Na J, Ying YJ, et al. Antiviral and anti-inflammatory activities of chemical constituents from twigs of mosla chinensis maxim. *Nat Prod Bioprospecting*. 2024;14(1):26. doi:10.1007/s13659-024-00448-w
44. Huang W, Wang C, Zhang H. Eriodictyol inhibits the motility, angiogenesis and tumor growth of hepatocellular carcinoma via NLRP3 inflammasome inactivation. *Heliyon*. 2024;10(3):e24401. doi:10.1016/j.heliyon.2024.e24401
45. Yan W, Changshu C, Tianrui Z, et al. Phytochemicals from anneslea fragrans Wall. and their hepatoprotective and anti-inflammatory activities. *Molecules*. 2023;28(14):5480. doi:10.3390/molecules28145480
46. Shan M, Xu X, Chu C, Wang H, Zhang C, Cai S. Ingredients in Rhus chinensis mill. fruits oil relieve fatigue by reducing oxidative damage and regulating energy metabolism and gut microbiota. *Food Biosci*. 2024;59:104099. doi:10.1016/j.fbio.2024.104099
47. Jian-Chun L, Shu-Yi L, Jian-Xian T, et al. Triterpenoids, steroids and other constituents from Euphorbia kansui and their anti-inflammatory and anti-tumor properties. *Phytochemistry*. 2022;204:113449. doi:10.1016/j.phytochem.2022.113449
48. Jin L, ShiHua D, Jing L, et al. Obacunone alleviates ferroptosis during lipopolysaccharide-induced acute lung injury by upregulating Nrf2-dependent antioxidant responses. *Cell Mol Biol Lett*. 2022;27(1):29. doi:10.1186/s11658-022-00318-8
49. Lei T, Jianxin C, Tianrui Z, Yaping L, Afsar K, Guiguang C. The bioavailability, extraction, biosynthesis and distribution of natural dihydrochalcone: phloridzin. *Int J Mol Sci*. 2021;22(2):962. doi:10.3390/ijms22020962
50. Ben BW, Retno NAD, Malak D, et al. Phytochemical profiling of the leaf extract of Ximenia americana var. caffra and its antioxidant, antibacterial, and antiaging activities in vitro and in Caenorhabditis elegans: a cosmeceutical and dermatological approach. *Oxid Med Cell Longev*. 2022;2022:3486257. doi:10.1155/2022/3486257
51. Hui S, QianYing L, Hui L, et al. ROS-induced oxidative stress is a major contributor to sperm cryoinjury. *Hum Reprod*. 2024;39(2):310–325. doi:10.1093/humrep/dead250

52. Galindo IF, Carmona SG, Ponce JA, et al. sRAGE levels are decreased in plasma and sputum of COPD secondary to biomass-burning smoke and tobacco smoking: differences according to the rs3134940 AGER variant. *Heliyon*. 2024;10(7):e28675. doi:10.1016/j.heliyon.2024.e28675
53. Xu R, Du W, Yang Q, Du A. ITGB2 related to immune cell infiltration as a potential therapeutic target of inflammatory bowel disease using bioinformatics and functional research. *J Cell Mol Med*. 2024;28(15):e18501. doi:10.1111/jcmm.18501
54. DI T, Angelo M, Michael N, et al. Receptor for advanced glycation end-products: biological significance and imaging applications. *Wiley Interdiscip Rev Nanomed Nanobiotechnol*. 2023;16(1):e1935. doi:10.1002/wnan.1935
55. Gutowska K, Koźniewski K, Wąsowski M, et al. AGER-1 long non-coding RNA levels correlate with the expression of the advanced glycosylation end-product receptor, a regulator of the inflammatory response in visceral adipose tissue of women with obesity and type 2 diabetes mellitus. *Int J Mol Sci*. 2023;24(24):17447. doi:10.3390/ijms242417447
56. Chanyuan L, Ting D, Junya C, et al. Identifying ITGB2 as a potential prognostic biomarker in ovarian cancer. *Diagnostics*. 2023;13(6):1169. doi:10.3390/diagnostics13061169
57. Te SH, Kok JWK, Luo R, et al. Coexistence of Synechococcus and Microcystis blooms in a tropical urban reservoir and their links with microbiomes. *Environ Sci Technol*. 2023;57(4):1613–1624. doi:10.1021/acs.est.2c04943
58. Akarsu H, Liljander AM, Lacasta A. Canine Staphylococcaceae circulating in a Kenyan animal shelter. *Microbiol Spectr*. 2024;12(2):e0292423. doi:10.1128/spectrum.02924-23